Ecological Indicators 135 (2022) 108512

Contents lists available at ScienceDirect

Ecological Indicators

journal homepage: www.elsevier.com/locate/ecolind

Original Articles

Global population densities, climate change, and the maximum monthly temperature threshold as a potential tipping point for high urban densities

Brice B. Hanberry

USDA Forest Service, Rocky Mountain Research Station, Rapid City, SD 57702, USA

ARTICLE INFO

Keywords:
CMIP6
Exurban
Heat
Mitigation
Suburban
Tipping point
Urban

ABSTRACT

Heat waves lasting days or weeks are among potential hazards expected to increase with climate change, but beyond heat waves, sustained temperatures may be incompatible with high urban population densities. I examined patterns of population density classes and exposure to maximum monthly temperature to identify where high urban population density classes were more at risk for prolonged heat than other density classes and if heat may have influenced high urban population densities during the recent past (1970–2000). Then, I considered exposure of population density classes to maximum monthly temperature during the near future (2021–2040, under the sustainability shared socio-economic pathway ssp1-2.6) and the long-range future (2081–2100, under fossil fuel-driven ssp5-8.5) for three general circulation models. Population densities generally increased with increasing maximum monthly temperature by country; the highest density urban class had the greatest exposure to heat for 82 out of 199 countries. By temperature zone, the hypertropical zone inverted the order such that population densities increased with decreasing maximum monthly temperature, indicating that concentrated populations generally did not develop at high maximum monthly temperatures ≥ 36 °C. The 36 °C maximum monthly temperature threshold corresponds to heat wave warnings, which typically consist of a few consecutive days. Therefore, 36 °C maximum monthly temperature may indicate the start of an inhospitable tipping point beyond which human civilization may not flourish. Most land area will exceed 36 °C maximum monthly temperature under the CanESM5 ssp5-8.5 scenario by 2081–2100. Adaptation is not sufficient to moderate sustained unrelenting heat and migration of human populations would be less feasible than mitigation to reduce carbon emissions.

1. Introduction

The world's human population is becoming more urban, resulting in increased population densities. The global urban population surpassed the global rural population for the first time during 2007 and the urban population reaching 54% of the global population, or 3.9 billion, during 2014 (United Nations, 2015). By 2050, the world's urban population is expected to grow from 54% to 66% urban (United Nations, 2015). Although all regions are expected to urbanize over the coming decades, increases will continue to be concentrated (i.e., 90%) in Asia and Africa. Due to the increasing proportion of urban populations, rural populations are expected to peak around 2020 at close to 3.4 billion and decline to 3.1 billion by 2050 (United Nations, 2015). About 65% of countries will experience rural population declines and no countries will have urban population contraction and rural population expansion. Future estimates depend on scenarios such as fertility trends, migration, and resource consumption, resulting in great divergence by 2100, according to the scenarios from shared socioeconomic pathways (Jiang and O'Neill 2017; Riahi et al. 2017; Chen et al. 2020; Gao and O'Neill 2020). Indeed, an additional uncounted factor is the recent coronavirus disease 2019 (COVID-19) pandemic, which may cause abandonment of high-density cities for less populated locations in some regions due to teleworking opportunities.

While compact urban design can produce the most efficient human footprint, unplanned urban expansion leads to rapid sprawl, pollution and environmental degradation, and elevated consumption patterns, including water use and carbon emissions. Urban dwellers in low-density urban and suburban areas consume more resources, including energy, per capita than rural dwellers (Seto et al. 2010; United Nations, 2015). Urban dwellers will experience climate change particularly through atmospheric warming and heatwaves. The urban heat island effect, which elevates temperatures due to less evaporative cooling and greater heat storage in roads and buildings along with heat generated from energy use, exacerbates urban warming compared to non-urban

E-mail address: brice.hanberry@usda.gov.

https://doi.org/10.1016/j.ecolind.2021.108512
Received 27 September 2021; Received in revised form 30 November 2021; Accepted 27 December 2021
Available online 30 December 2021

areas. Urban areas may be 4.3 °C greater in the summer than non-urban surroundings, although cities in deserts and arid shrublands may exhibit, conversely, a heat sink (Imhoff et al. 2010).

Heat may cause heat stroke and trigger pulmonary and cardiovascular diseases. Hot weather contributes to greater ground-level ozone (smog) in polluted areas, wildfire smoke, and production of pollen, exacerbating respiratory problems. Dehydration from hot conditions may produce renal failure and cardiovascular complications. Warming may increase annual mortality rates by 5.4 (±0.5) deaths per 100,000 per °C in warming (Hsiang et al. 2017). Projected impacts of climate change on mortality vary with future demographic scenarios and climate models (Sanderson et al. 2017; Jones et al. 2018).

The spatial distribution of population densities can either intensify or relieve sustained exposure of populations to heat, but at some threshold, sustained heat may restrain population densities. Here, I assessed patterns of human population density, in five classes ranging from wildlands to urban high density, and heat exposure in temperature zones and countries by examining maximum monthly temperature during the recent past (1970–2000), near future (2021–2040), and the long-range future (2081–2100) with realized density classes (year 2000 and 2020), rather than unknown future demographic patterns. For near future climate as a starting point, I selected the sustainability shared socio-economic pathway 1–2.6 during 2021–2040, and to determine the maximum end point, I selected the greatest expected temperature increase of the fossil-fueled shared socio-economic pathway 5–8.5 (albeit measured carbon emissions typically exceed fossil-fueled projections) during 2081–2100. With this assessment to inform climate change risk, I located where high urban population densities had greatest heat exposure and the potential tipping point of maximum sustained heat that may restrict high urban population densities, indicating tolerance beyond human societies.

2. Methods

For global population densities, I used population counts during 2000 and 2020 from Worldpop, which populates census data throughout census blocks (i.e., dasymetric modeling using random forests regression) with model variables including land cover, urban land use, transportation networks and travel times, precipitation, slope, topography, and nighttime lights (cell size of 0.0083°, 30 s; Stevens et al. 2015; Lloyd et al. 2017; WorldPop, 2018). Worldpop is the only population model available for comparison during years 2000 and 2020. Population counts are meant to remain unprojected in the geographic coordinate system (GCS, or longitude and latitude) WGS 1984 to prevent distortion (Bright et al. 2016). I estimated cell areas in square kilometers for subsequent calculation of population density (Hijmans and van Etten 2012). I generated a calibrated classification of population density classes by matching urban percentage of Worldpop 2015 to the United Nations, 2015 global urban population estimate of 53.9% derived from census data (United Nations, 2021) and then balancing among four 2015 population models to reach approximately the same population percentages for wildlands and rural, exurban, suburban, urban low, and urban high density classes by density thresholds, which varied by dispersion of population models. For Worldpop, I classed population densities by pixel cell of 0 to 15 inhabitants per km^2 as wildlands and rural, 15 to 250 as exurban, 250 to 800 as suburban, 800 to 1900 as urban low density, and > 1900 as urban high density.

I also developed eight temperature zones based on number of growing degrees days > 0 °C, which is the sum of mean monthly temperature for months with mean temperature>0 ℃ multiplied by number of days (from ENVIREM 2020 derived from WorldClim 1.4, years 1960 to 1990, resolution of 0.042°; Hijmans et al. 2005; Title and Bemmels 2018). These zones matched well (i.e., 86% similar, with some indications of class improvement in unmatched zones) with the equivalent Köppen primary thermal climate classes of polar, tundra, boreal, temperate warm, temperate hot, subtropical, and tropical; development of these zones provided flexibility in adding a hypertropical class (≥11,500 growing degree days at base 0 °C) and not masking thermal classes with aridity classes. I held temperature zones constant over time.

For climate, I used maximum temperature of the warmest month during recent past of years 1970 to 2000, current to near future of 2021 to 2040, and 2081 to 2100 (WorldClim 2.1, WorldClim 2020; resolution of 0.042°, 2.5 min; Fick and Hijmans 2017). For WorldClim 2.1, Fick and Hijmans (2017) downscaled climate data using covariables and the thin-plate smoothing spline algorithm; all temperature variables had a global correlation coefficient between estimated and observed values of ≥ 0.99. Although climate data for future years were available at 0.042° but not 0.0083° resolution, maximum temperature of the warmest month during years 1970 to 2000 was available at 0.0083° resolution and when summarized, values were the same as at 0.042° resolution. Regarding emission scenarios from Coupled Model Intercomparison Project phase 6 (CMIP6), I selected the shared socio-economic pathway of least climate departure for years 2021–2040, ssp1-2.6, and for years 2081–2100, I selected the shared socio-economic pathway of greatest climate departure, ssp5-8.5. The Coupled Model Intercomparison Project coordinates global climate model simulations of the past, current, and future climate under radiative forcing; phase 6 better addresses issues such as impact of short-term forcing agents and land use on climate and decadal variability than phase 5 (Eyring et al., 2016; World Climate Research Programme 2021). The shared socio-economic pathway are reference cases for mitigation, climate impacts, and adaptation analyses; the sustainability pathway (ssp1-2.6) shifts focus from economics to overall well-being, with low resource and energy consumption, whereas the fossil-fueled pathway (ssp5-8.5) involves confidence in technological innovation combined with resource and energy intensive lifestyles (Riahi et al. 2017). As for general circulation models, I used Canadian Earth System Model version 5 (CanESM5; Swart et al. 2019), Model for Interdisciplinary Research on Climate, Earth System version 2 for Long-term simulations (MIROC-ES2L; Hajima et al. 2020) and Meteorological Research Institute Earth System Model version 2.0 (MRI-ESM2-0, Yukimoto et al. 2019), which provided full coverage of all counties and population density classes.

I applied zonal statistics (ESRI, ArcMap v. 10.5.1, West Redlands, CA) to determine mean values of the maximum temperature of the warmest month for population densities by global land area, by temperature zone, or by country for each time interval and general circulation models. I used population density classes during 2000 for the recent past of 1970 to 2000 and population density classes during 2020 for the future time intervals of 2021 to 2040 and 2081 to 2100. I identified zones where heat appeared to restrict increases in population densities. By country, I compared the hottest temperature of the greatest density urban class, which typically was urban high density although not for all countries, to other density classes to identify countries where the urban highest density class was most vulnerable to heat risk.

3. Results

For temperature zones, the polar and tundra zones primarily were wildlands and rural, which caused depression of temperatures in the wildlands and rural population density class globally (Fig. 1; Table 1). Population densities increased with increasing maximum monthly temperature during the recent past (1970–2000) in the boreal zone, which indicated a positive response by human densities to warmer locations (Fig. 2). Population density classes also increased with increasing maximum monthly temperature in the temperate warm zone, except the wildlands-rural class was located in warmer locations than the other population density classes. For the temperate hot, subtropical, and tropical zones, greater maximum monthly temperature occurred in the suburban and the urban low-density classes compared to the urban high-density class and exurban class. However, in the hypertropical zone, population densities decreased with increasing maximum monthly temperature from the urban high-density class (35.25 °C), urban low-

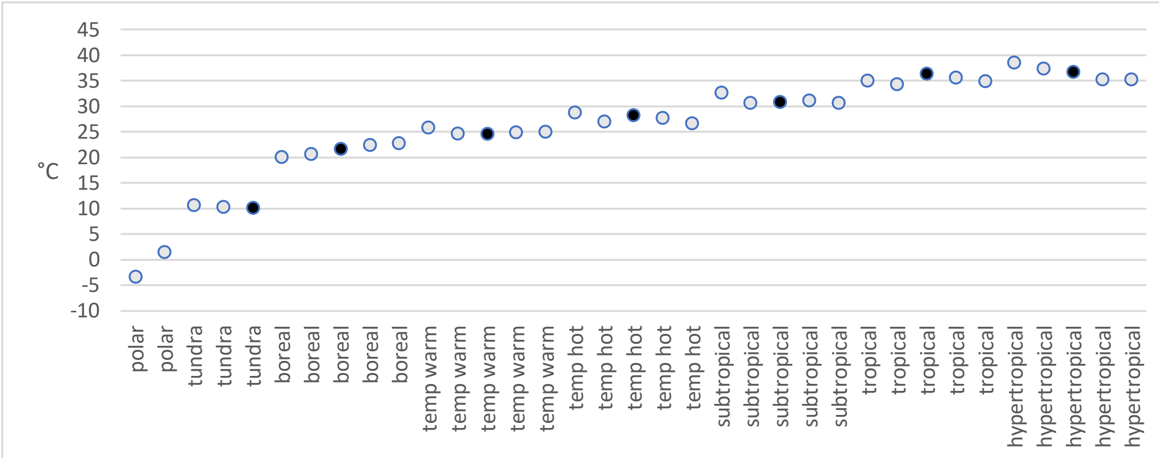

Fig. 1. Maximum monthly temperature (°C) by population density classes of wildlands and rural, exurban, suburban (black color), urban low, and urban high by temperature zones during the recent past (1970–2000).

Table 1
Number of cells and area (km^2) of population density classes during 2000 by thermal zone.

Zone	Density class	Number of cells	Area
polar	wildlands-rural	7,776,400	1646649.71
polar	exurban	175	136.69
tundra	wildlands-rural	20,905,150	6526149.82
tundra	exurban	5700	3422.21
tundra	suburban	225	82.20
boreal	wildlands-rural	52,567,675	23243111.60
boreal	exurban	802,575	412878.67
boreal	suburban	35,500	16303.12
boreal	urban low	9225	4263.49
boreal	urban high	4350	2037.14
temp warm	wildlands-rural	20,502,750	11689336.19
temp warm	exurban	4,874,700	2811121.46
temp warm	suburban	315,750	176465.14
temp warm	urban low	90,050	49844.07
temp warm	urban high	62,025	33924.50
temp hot	wildlands-rural	11,677,975	7591990.85
temp hot	exurban	5,476,075	3529221.44
temp hot	suburban	877,350	568176.36
temp hot	urban low	238,175	149514.11
temp hot	urban high	138,550	84733.86
subtropical	wildlands-rural	22,304,525	16681658.87
subtropical	exurban	6,737,375	5108180.80
subtropical	suburban	1,285,825	953597.76
subtropical	urban low	299,000	218505.25
subtropical	urban high	174,500	127310.38
tropical	wildlands-rural	35,665,000	29041625.12
tropical	exurban	8,046,200	6578571.38
tropical	suburban	1,411,375	1109114.67
tropical	urban low	410,625	322374.17
tropical	urban high	124,800	98713.61
hypertropical	wildlands-rural	12,554,825	10382960.46
hypertropical	exurban	4,435,000	3686827.67
hypertropical	suburban	624,975	513968.92
hypertropical	urban low	131,000	108692.52
hypertropical	urban high	56,725	47184.21

density class (35.33 °C), suburban class (36.8 °C), and exurban density class (37.3 °C). This indicates a negative response of human populations to prolonged heat. Although hyperarid conditions also may curtail dense populations, the hypertropical zone extended beyond hyperarid locations (Fig. 2). Urban populations by zone only occurred below a maximum monthly temperature 36 °C, albeit cities are present above this threshold. Under the CanESM5 ssp5-8.5 model, most inhabited land will exceed the 36 °C maximum monthly temperature threshold during 2081 to 2100 (Fig. 3), while the other general circulation models likely would follow these projections during the early 2100s.

For all global area, maximum monthly temperature was greatest in the suburban and urban low classes, followed by the urban high class, exurban class, and wildlands and rural class for all time intervals and general circulation models (Fig. 4). The CanESM5 general circulation model had the greatest temperatures for population densities. The MIROC-ES2L and MRI-ESM2-0 models had similar temperatures for population densities.

By country, the maximum monthly temperature increased consistently with increasing population density classes (exurban, suburban, urban low, urban high) and over time (Fig. 5). This divergence of pattern from global land area is due to equal weighting of numerous small countries. For the recent past and near future, the maximum monthly temperature in the urban high-density class was about 0.85 °C greater than the exurban densities. This difference increased to about 1 °C by 2081–2100. Therefore, most countries will have the greatest heat risk where populations are most concentrated.

The highest density urban class, whether the urban high-density or urban low-density class, was cooler in maximum monthly temperature during 1970–2000 than one or more other classes for 117 out of 199 countries (with urban density classes during 2000), whereas greatest heat exposure occurred for the most concentrated populations of 82 countries (Fig. 6). For the general circulation models during 2081–2100, the highest density urban class was cooler in maximum monthly temperature than one or more other classes for 121 (MIROC-ES2L and CanESM5) and 124 (MRI-ESM2-0) out of 210 countries (with urban density classes during 2020; Fig. 7). That is, 86 to 89 countries may have concentrated populations with most exposure to prolonged heat.

4. Discussion

4.1. Central findings

The highest density urban class had the greatest exposure of the population density classes to heat for 82 out of 199 countries and maximum monthly temperature in the urban high-density class was about 0.85 °C greater than the exurban low densities for countries. Countries that are most at risk for heat waves and sustained maximum temperatures have the highest urban density populations located in warmer locations than exurban populations. In contrast, countries with highest urban density populations sited in cooler locations may help offset the urban heat island effect and warming temperatures.

However, by temperature zones, the hypertropical zone inverted the trend such that population densities decreased from urban high density, urban low density, suburban, to exurban classes with increased

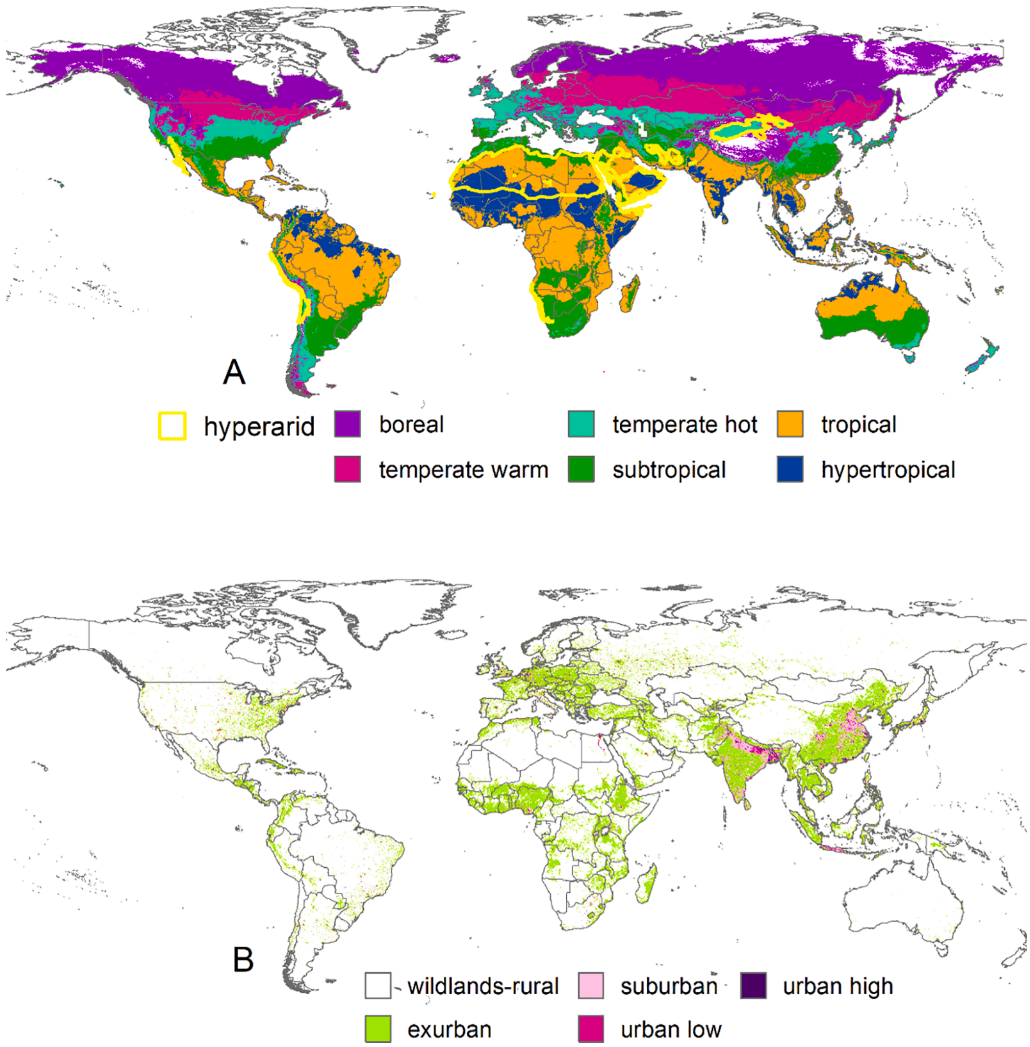

Fig. 2. Thermal zones including the boreal zone, where population densities increased with increasing maximum monthly temperature, and the hypertropical zone, where population densities decreased with increasing maximum monthly temperature, with hyperarid locations delineated (A) and population density classes of wildlands and rural (0 to 15 humans per km^2), exurban (15 to 250 humans per km^2), suburban (250 to 800 humans per km^2), urban low density (800 to 1900 humans per km^2), and urban high density (>1900 humans per km^2; B). (Figures are in the WGS 1984 geographic coordinate system.)

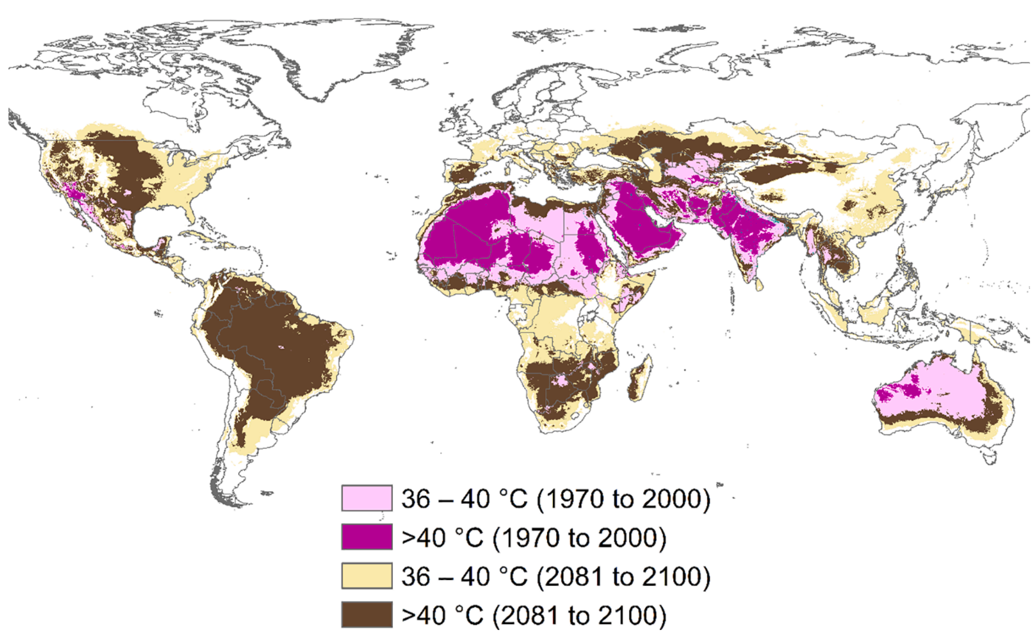

Fig. 3. Most inhabited land will cross the 36 °C maximum monthly temperature threshold by 2081–2100 under the CanESM5 scenario. (Figure is in the WGS 1984 geographic coordinate system.)

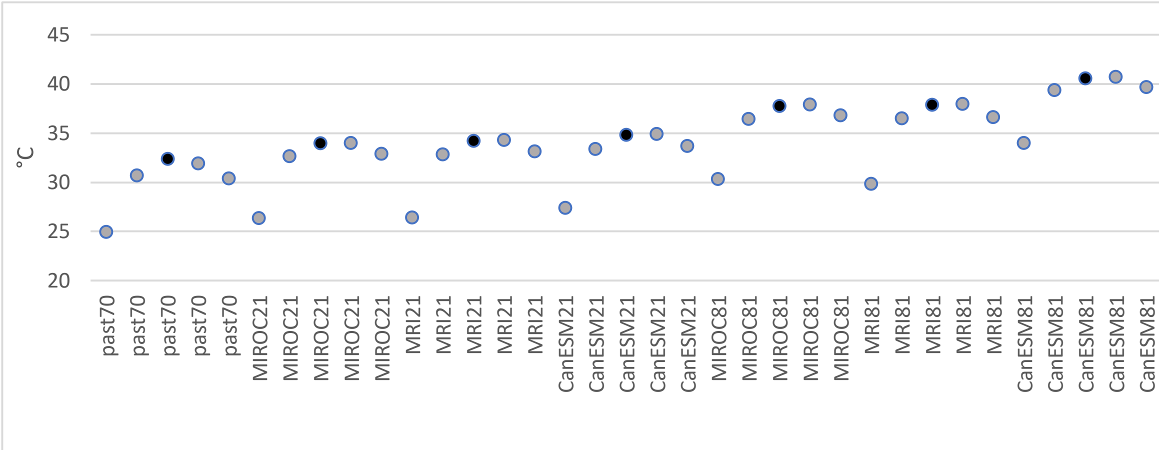

Fig. 4. Maximum monthly temperature (°C) for global land area by population density classes of wildlands and rural, exurban, suburban (black color), urban low, and urban high during the recent past (1970–2000); MIROC-ES2L, MRI-ESM2-0, and CanESM5 during 2021 to 2040; and MIROC-ES2L, MRI-ESM2-0, and CanESM5 during 2081–2100.

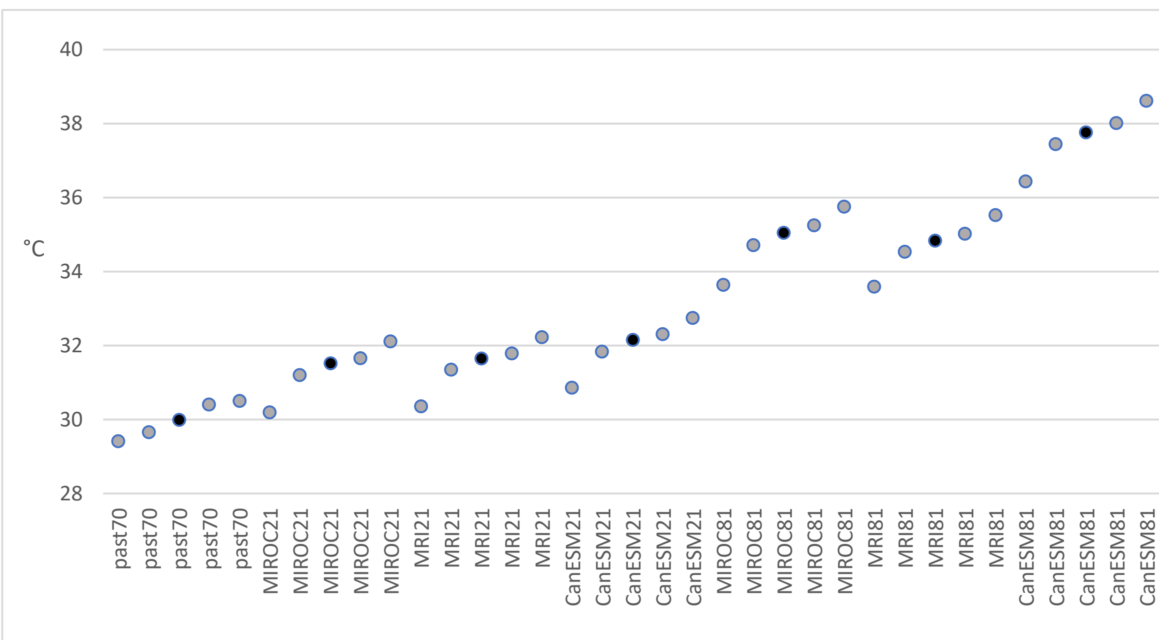

Fig. 5. Maximum monthly temperature (°C) for countries by population density classes of wildlands and rural, exurban, suburban (black color), urban low, and urban high during the recent past (1970–2000); MIROC-ES2L, MRI-ESM2-0, and CanESM5 during 2021 to 2040; and MIROC-ES2L, MRI-ESM2-0, and CanESM5 during 2081–2100.

maximum monthly temperature. This inversion, with urban populations overall located below 36 °C maximum monthly temperature, may indicate a tipping point beyond which human populations will not prosper. Maximum temperatures of about 36 °C match well with heat wave warnings for countries that use temperature as the alert criterion, although typically based on a few consecutive days, not an entire month (Lee et al., 2016). Warnings by country range from daily maximum temperatures $\geq$ 25 °C for five consecutive days in the Netherlands to daily maximum temperatures $\geq$ 40 °C for three consecutive days in Australia, where the majority of the population avoids the hotter, northern portions of the country (Lee et al., 2016). Mortality may occur due to consecutive days of moderately hot and humid weather with daily maximum temperatures of 28 °C to 32 °C (Lee et al., 2016).

If this threshold of 36 °C is within the starting range (e.g., 36 °C to 40 °C) of prolonged heat intolerable for human populations to flourish, major heat-related problems may occur by 2081–2100 for most land area, which will exceed the maximum monthly temperature $\geq$ 36 °C under the CanESM5 model and fossil fuel-driven ssp5-8.5 scenario (Fig. 3). The number of countries that cross this threshold will increase from 23 to about 85 to 90 countries for MIROC-ES2L and MRI-ESM2-0 models and 140 countries for the CanESM5 model. Albeit less consequential in the face of comprehensive, sustained heat beyond temporary heat waves, the number of countries with a cooler highest density urban class remained relatively stable over time.

Caveats included that while the impacts of hot temperatures were indicated by maximum monthly temperature, the most appropriate index remains unknown (Lee et al., 2016). Heat wave anomalies that are greater than temperatures to which populations are acclimated or heat stress with inclusion of relative humidity may be better indices. The duration of the heat wave also is important (Lee et al., 2016). Nonetheless, twenty-year means of increasingly warming maximum monthly temperature is a not an anomaly, which prompts a range of responses

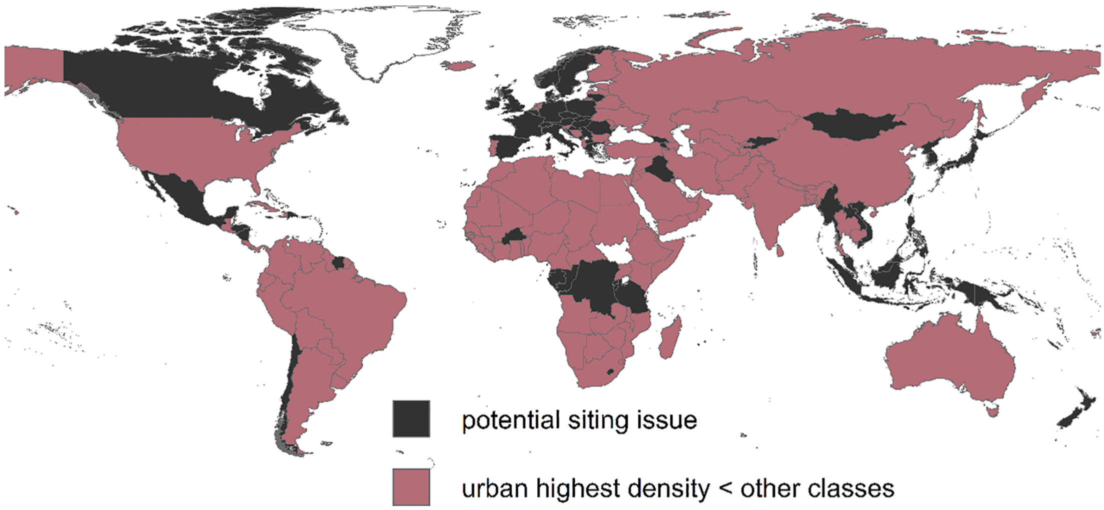

Fig. 6. The highest density urban class was cooler in maximum monthly temperature than one or more other residential classes during 1970–2000 for 117 out of 199 countries with urban density classes (during 2000). Problems may occur where the highest density urban class was sited in the hottest maximum monthly temperature. (Figure is in the WGS 1984 geographic coordinate system.)

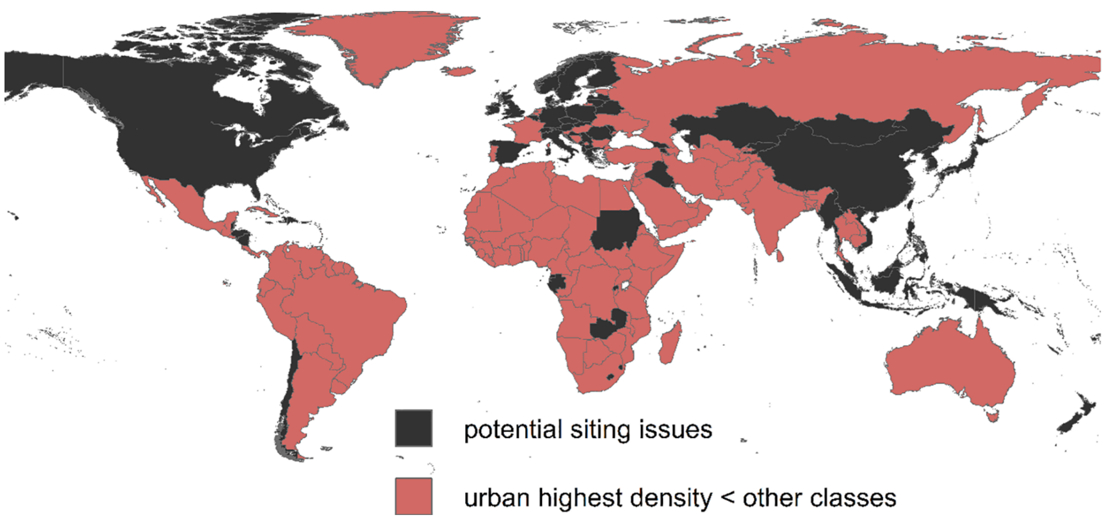

Fig. 7. The highest density urban class was cooler in maximum monthly temperature than one or more other residential classes during 2081–2100 (MIROC-ES2L general circulation model) for 121 out of 210 countries with urban density classes (during 2020). Problems may occur where the highest density urban class was sited in the hottest maximum monthly temperature. (Figure is in the WGS 1984 geographic coordinate system.)

beyond morbidity and mortality.

Additionally, I applied climate projections for 2081 to 2100 but held populations fixed at 2020, given that urban infrastructure is in place. Indeed, it may be unnecessary to examine population dynamics given that the land extent of future climate change will be comprehensive, with most populations experiencing maximum monthly temperatures in excess of 36 °C (Fig. 3). Uncertainty in estimates also originates from general circulation models, scenarios, and downscaling, but continuing along the shared socio-economic pathway 5–8.5 of carbon emissions, temperatures eventually may become unsustainable for current human society.

4.2. Implications

Climate change is affecting ecosystems and societies in numerous ways, including increased heat waves. Currently, hot temperatures may compromise health and outside activities of both work and leisure. Deferral of action can occur because climate change is slow to develop, until it is too late to prevent. Shifting baselines may cause increased tolerance for progressive escalation of warming intensity. Climate change will be past the early warning signs when maximum monthly temperatures surpass 36 °C throughout most of the global land area, perhaps 70 years from now.

Adaptation strategies can reduce exposure and mitigation can reduce climate change. Humans have adapted to heat by using air conditioning units, but this use contributes to increased climate warming if the energy used is not renewable (Barreca et al. 2016). Residents, communities, nations, and the world have delayed employing comprehensive adaptation and mitigation strategies to reduce vulnerability to climate change and switch reliance from fossil fuels to renewable energy, despite long-term economic, social, and ecological benefits.

Based on the widespread extent of intolerable maximum monthly temperatures on the current fossil fuel-driven pathway, planning for most efficient fossil fuel use will not be sufficient to shift our trajectory, albeit improved energy efficiency measures (e.g., buildings, appliances) and high-density populations can reduce carbon emissions (Griffith et al. 2020). Providing services in well-planned, high-density cities is typically less expensive (i.e., economies of scale or density) and less environmentally damaging than providing similar services to dispersed rural populations (United Nations, 2015). Well-planned cities also provide greater livability, health, justice, equality, and resilience (United Nations, 2015).

Climate change is expected to cause migration from areas of heat (Partridge et al. 2017). Temporary and permanent migration is a tool for households with food and livelihood insecurity to gain these securities. Climate-related migration appears to be likely for both those with means and those without (Partridge et al. 2017). Nevertheless, it also seems unlikely that billions of people can or will move, and this option is likely be more costly and challenging than mitigation.

Embarking on atmospheric carbon drawdown and net-zero carbon emissions by 2050 is possible through existing technologies of rapid electrification based on renewable energy: wind and solar power plants, rooftop solar, electric vehicles, heat pumps, and batteries (Griffith et al. 2020). For the United States to achieve net-zero carbon emissions by 2050, total government share of the expense is estimated at only $250–350 billion per year (Griffith et al. 2020), which is less government investment than that required for World War II, which resulted in an economic boom. While the cited costs might be underestimates, changing the pathway maybe less expensive than trying to live in an increasingly adverse climate. Electrification can occur without sacrifice to downsized homes and reduced driving of personal cars. Solar and wind power are more economical than fossil fuels, particularly with overbuilding to distributed energy grids rather than concentrated utility-scale power generators (Perez et al. 2019; Clack et al. 2020).

5. Conclusions

We cannot adapt our way out of temperature increases of our current fossil fuel-driven shared socio-economic pathway and migration of most of the human population is not a viable option. For most countries, the highest density urban class was sited in the hottest location or will exceed 36 °C maximum monthly temperature. These countries will face the greatest challenges for planning and may have the greatest migration in response to climate change. Given the current pathway, the present analysis indicated that most land area may tip beyond a maximum monthly temperature of 36 °C by 2081–2100, or at best, this conclusion may be deferred until the early 2100s. Every density class will be vulnerable, but the highest density class may be the first to cross the maximum monthly temperature threshold. Rapid decarbonization using existing technologies is necessary to alter the trajectory from the maximum monthly temperature threshold, which will impose ecological and socio-economic costs of climate damage.

Declaration of Competing Interest

The authors declare that they have no known competing financial interests or personal relationships that could have appeared to influence the work reported in this paper.

Acknowledgement

I thank the anonymous reviewers. This research was supported by the USDA Forest Service, Rocky Mountain Research Station. The findings and conclusions in this publication are those of the author and should not be construed to represent any official USDA or U.S. Government determination or policy. I acknowledge the World Climate Research Programme, which, through its Working Group on Coupled Modelling, coordinated and promoted CMIP6. I recognize the climate modeling groups for producing and making available their model output and multiple funding agencies who supported CMIP6.

References

Barreca, A., Clay, K., Deschenes, O., Greenstone, M., Shapiro, J.S., 2016. Adapting to climate change: The remarkable decline in the US temperature-mortality relationship over the twentieth century. Journal of Political Economy 124 (1), 105–159.

Bright, E.A., Rose, A.N., Urban, M.L., 2016. LandScan 2015. Oak Ridge National Lab, Oak Ridge, TN. Available at https://landscan.ornl.gov/. Accessed 28 February 2021.

Chen, G., Li, X., Liu, X., Chen, Y., Liang, X., Leng, J., Xu, X., Liao, W., Qiu, Y., Wu, Q., Huang, K., 2020. Global projections of future urban land expansion under shared socioeconomic pathways. Nat. Commun. 11 (1) https://doi.org/10.1038/s41467-020-14386-x.

Clack, C. T. M., Choukulkar, A., Coté, B., and McKee, S. A. 2020. Why local solar for all costs less: A new roadmap for the lowest cost grid. Vibrant Clean Energy, Boulder, Colorado. Available at: https://www.vibrantcleanenergy.com/wpcontent/uploads/2020/12/WhyDERs_TR_Final.pdf. Accessed 31 July 2021.

Eyring, V., Bony, S., Meehl, G.A., Senior, C.A., Stevens, B., Stouffer, R.J., Taylor, K.E., 2016. Overview of the Coupled Model Intercomparison Project Phase 6 (CMIP6) experimental design and organization. Geosci. Model Dev. 9 (5), 1937–1958.

ENVIREM. 2020. ENVIREM: ENVIronmental Rasters for Ecological Modeling version 1.0. Available at: https://deepblue.lib.umich.edu/data/concern/data_sets/gt54kn05f Accessed 23 February 2021.

Gao, J., O'Neill, B.C., 2020. Mapping global urban land for the 21st century with data-driven simulations and Shared Socioeconomic Pathways. Nat. Commun. 11, 1–12.

S. Griffith S. Calisch L. Fraser Rewiring America, a handbook for winning the climate fight Available at https://www.rewiringamerica.org/handbook 2020 Accessed 31 July 2021.

Fick, S.E., Hijmans, R.J., 2017. WorldClim 2: new 1km spatial resolution climate surfaces for global land areas. Int. J. Climatol. 37 (12), 4302–4315.

Hajima, T., Watanabe, M., Yamamoto, A., Tatebe, H., Noguchi, M.A., Abe, M., Ohgaito, R., Ito, A., Yamazaki, D., Okajima, H., Ito, A., Takata, K., Ogochi, K., Watanabe, S., Kawamiya, M., 2020. Development of the MIROC-ES2L Earth system model and the evaluation of biogeochemical processes and feedbacks. Geosci. Model Dev. 13 (5), 2197–2244.

Hijmans, R.J., Cameron, S.E., Parra, J.L., Jones, P.G., Jarvis, A., 2005. Very high resolution interpolated climate surfaces for global land areas. International Journal of Climatology: A Journal of the Royal Meteorological Society 25 (15), 1965–1978.

R.J. Hijmans J. van Etten raster: Geographic analysis and modeling with raster data Available at: http://CRAN.R-project.org/package=raster 2012 Accessed 1 January 2021.

Hsiang, S., Kopp, R., Jina, A., Rising, J., Delgado, M., Mohan, S., Rasmussen, D.J., Muir-Wood, R., Wilson, P., Oppenheimer, M., Larsen, K., Houser, T., 2017. Estimating economic damage from climate change in the United States. Science 356 (6345), 1362–1369.

Imhoff, M.L., Zhang, P., Wolfe, R.E., Bounoua, L., 2010. Remote sensing of the urban heat island effect across biomes in the continental USA. Remote Sens. Environ. 114 (3), 504–513.

Jiang, L., O'Neill, B.C., 2017. Global urbanization projections for the Shared Socioeconomic Pathways. Global Environ. Change 42, 193–199.

Jones, B., Tebaldi, C., O'Neill, B.C., Oleson, K., Gao, J., 2018. Avoiding population exposure to heat-related extremes: demographic change vs climate change. Clim. Change 146 (3-4), 423–437.

Lee, J.-S., Byun, H.-R., Kim, D.-W., 2016. Development of accumulated heat stress index based on time-weighted function. Theor. Appl. Climatol. 124 (3-4), 541–554.

Lloyd, C.T., Sorichetta, A., Tatem, A.J., 2017. High resolution global gridded data for use in population studies. Sci. Data 4, 1–17.

Partridge, M.D., Feng, B.o., Rembert, M., 2017. Improving climate-change modeling of US migration. American Economic Review 107 (5), 451–455.

Perez, M., Perez, R., Rábago, K.R., Putnam, M., 2019. Overbuilding & curtailment: The cost-effective enablers of firm PV generation. Sol. Energy 180, 412–422.

Riahi, K., van Vuuren, D.P., Kriegler, E., Edmonds, J., O'Neill, B.C., Fujimori, S., Bauer, N., Calvin, K., Dellink, R., Fricko, O., Lutz, W., Popp, A., Cuaresma, J.C., KC, S., Leimbach, M., Jiang, L., Kram, T., Rao, S., Emmerling, J., Ebi, K., Hasegawa, T., Havlik, P., Humpenöder, F., Da Silva, L.A., Smith, S., Stehfest, E., Bosetti, V., Eom, J., Gernaat, D., Masui, T., Rogelj, J., Strefler, J., Drouet, L., Krey, V., Luderer, G., Harmsen, M., Takahashi, K., Baumstark, L., Doelman, J.C., Kainuma, M., Klimont, Z., Marangoni, G., Lotze-Campen, H., Obersteiner, M., Tabeau, A., Tavoni, M., 2017. The Shared Socioeconomic Pathways and their energy, land use, and greenhouse gas emissions implications: An overview. Global Environ. Change 42, 153–168.

Sanderson, M., Arbuthnott, K., Kovats, S., Hajat, S., Falloon, P., Añel, J.A., 2017. The use of climate information to estimate future mortality from high ambient temperature: a systematic literature review. PLoS ONE 12 (7), e0180369.

Seto, K.C., Sánchez-Rodríguez, R., Fragkias, M., 2010. The new geography of contemporary urbanization and the environment. Annu. Rev. Environ. Resour. 35 (1), 167–194.

Stevens, F.R., Gaughan, A.E., Linard, C., Tatem, A.J., Amaral, L.A.N., 2015. Disaggregating census data for population mapping using random forests with remotely-sensed and ancillary data. PLoS ONE 10 (2), e0107042.

Swart, N.C., Cole, J.N.S., Kharin, V.V., Lazare, M., Scinocca, J.F., Gillett, N.P., Anstey, J., Arora, V., Christian, J.R., Hanna, S., Jiao, Y., Lee, W.G., Majaess, F., Saenko, O.A., Seiler, C., Seinen, C., Shao, A., Sigmond, M., Solheim, L., von Salzen, K., Yang, D., Winter, B., 2019. The Canadian earth system model version 5 (CanESM5.0.3). Geosci. Model Dev. 12 (11), 4823–4873.

Title, P.O., Bemmels, J.B., 2018. ENVIREM: an expanded set of bioclimatic and topographic variables increases flexibility and improves performance of ecological niche modeling. Ecography 41 (2), 291–307.
United Nations, Department of Economic and Social Affairs, Population Division. 2015. World urbanization prospects: The 2014 revision. ST/ESA/SER.A/366. New York: United Nations. Available at https://population.un.org/wup/Publications/Files/WUP2014-Report.pdf Accessed 29 July 2021.
United Nations, Department of Economic and Social Affairs, Population Division Urban and rural populations Available at: https://worldclim.org/data/cmip6/cmip6climate.html/ 2021 Accessed 1 September 2021.
WorldClim Future climate data Available at https://population.un.org/wup/Publications/Files/WUP2014-Report.pdf 2020 Accessed 25 February 2021.
WorldPop (www.worldpop.org - School of Geography and Environmental Science, University of Southampton; Department of Geography and Geosciences, University of Louisville; Departement de Geographie, Universite de Namur) and Center for International Earth Science Information Network (CIESIN), Columbia University. 2018. Global High Resolution Population Denominators Project - Funded by The Bill and Melinda Gates Foundation (OPP1134076).
World Climate Research Programme CMIP Phase 6 (CMIP6) Available at: https://www.wcrp-climate.org/wgcm-cmip/wgcm-cmip6 2021 Accessed November 27, 2021.
Yukimoto, S., Kawai, H., Koshiro, T., Oshima, N., Yoshida, K., Urakawa, S., Tsujino, H., Deushi, M., Tanaka, T., Hosaka, M., Yabu, S., 2019. The Meteorological Research Institute Earth System Model version 2.0, MRI-ESM2. 0: Description and basic evaluation of the physical component. Journal of the Meteorological Society of Japan. Ser. II. 97, 931–965.